

Observation of ferromagnetic resonance in the time domain

R. J. Hicken and J. Wu

Citation: *J. Appl. Phys.* **85**, 4580 (1999); doi: 10.1063/1.370414

View online: <http://dx.doi.org/10.1063/1.370414>

View Table of Contents: <http://jap.aip.org/resource/1/JAPIAU/v85/i8>

Published by the [American Institute of Physics](#).

Related Articles

Enhanced spin pumping damping in yttrium iron garnet/Pt bilayers
Appl. Phys. Lett. **102**, 012402 (2013)

Mapping microwave field distributions via the spin Hall effect
Appl. Phys. Lett. **101**, 252406 (2012)

Enhancing exchange bias and tailoring microwave properties of FeCo/MnIr multilayers by oblique deposition
J. Appl. Phys. **112**, 113908 (2012)

Transmission of microwaves through exchange-coupled bi-layer magnetic films in ferromagnetic and standing spin wave resonances
J. Appl. Phys. **112**, 093901 (2012)

Room temperature microwave-assisted recording on 500-Gbps-class perpendicular medium
J. Appl. Phys. **112**, 083912 (2012)

Additional information on J. Appl. Phys.

Journal Homepage: <http://jap.aip.org/>

Journal Information: http://jap.aip.org/about/about_the_journal

Top downloads: http://jap.aip.org/features/most_downloaded

Information for Authors: <http://jap.aip.org/authors>

ADVERTISEMENT



AIP Advances

Now Indexed in Thomson Reuters Databases

Explore AIP's open access journal:

- Rapid publication
- Article-level metrics
- Post-publication rating and commenting

Observation of ferromagnetic resonance in the time domain

R. J. Hicken and J. Wu

School of Physics, University of Exeter, Stocker Road, Exeter EX4 4QL, United Kingdom

Optical pump–probe spectroscopy has been used to observe damped ferromagnetic resonance (FMR) oscillations in thin film Fe samples. The FMR was pumped by magnetic field pulses generated by an optically triggered photoconductive switch, and probed by means of time resolved measurements of the magneto-optical Kerr rotation. The photoconductive switch structure consisted of a parallel wire transmission line, of $125\ \mu\text{m}$ track width and separation, defined on a semi-insulating GaAs substrate. The biased transmission line was optically gated at one end so that a current pulse propagated along the transmission line to where the sample had been overlaid. The magnetic field associated with the current pulse is spatially nonuniform. By focusing the probe beam on the sample at different points above the transmission line the effect of the orientation of the pump field has been studied. The gyroscopic motion of the magnetization has been modeled by solving the Landau–Lifshitz–Gilbert equation and the magneto-optical response of the sample has been calculated by taking account of both the longitudinal and polar Kerr effects. The calculated and measured magneto-optical Kerr rotations are found to be in reasonable agreement. © 1999 American Institute of Physics. [S0021-8979(99)78608-1]

I. INTRODUCTION

It has recently been shown that optical pump–probe spectroscopy can be used to observe dynamical magnetic processes in thin film ferromagnetic samples on picosecond time scales.^{1–3} The sample is pumped by a magnetic field pulse generated by a photoconductive switch and the response of the magnetization is probed by means of a time resolved measurement of the magneto-optical Kerr rotation. In this article we explore how the orientation of the pulsed magnetic field affects the subsequent motion of the magnetization and hence the observed magneto-optical response of the sample.

II. EXPERIMENT

The optical pump–probe apparatus used to observe the FMR is shown in schematic form in Fig. 1. A mode-locked Ti:Al₂O₃ laser was used to generate 100 fs pulses at a wavelength of 800 nm, a repetition rate of 82 MHz, and an average power of about 800 mW. Each pulse was divided into pump and probe parts by a 90/10 beam splitter and the *p*-polarized probe beam was intensity stabilized⁴ to 0.1%. The pump and probe beams were focused with lenses of focal length 15 cm and 8 cm, respectively, giving a probe spot diameter of approximately $50\ \mu\text{m}$. The time delay between the pump and probe pulses at the sample was varied by reflecting the pump beam from a corner cube reflector mounted on a stepper motor-driven translation stage. The sample was placed on top of a photoconductive switch structure such as that shown in Fig. 2. This was then mounted on a small translation stage so that the position of the probe spot on the sample could be easily adjusted. An electromagnet

was used to apply a static magnetic field either parallel or perpendicular to the plane of incidence of the probe beam at the sample. The detector consisted of a Glan–Thompson polarizing beam splitter and two photodiode detectors that formed an optical bridge. The magneto-optical Kerr effect (MOKE) causes the reflected probe beam to be elliptically polarized. The difference of the two photodiode outputs is proportional to the rotation of the major axis of the ellipse. Light from a 633 nm HeNe laser was added to the main beam to aid alignment of the apparatus.

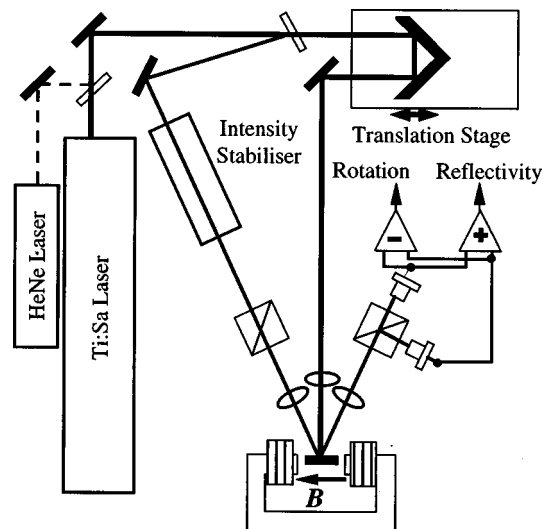


FIG. 1. Schematic representation of the optical pump–probe apparatus.

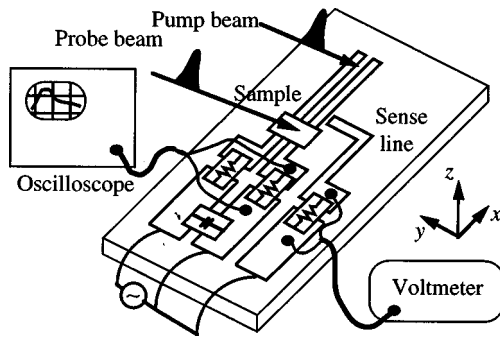


FIG. 2. The photoconductive switch structure is shown in schematic form.

The design of the photoconductive switch structure is shown in Fig. 1 and is similar to that used in Refs. 1 and 2. A Au transmission line of 125 μm track width and separation, and thickness of order 0.1 μm , was lithographically defined on an intrinsic semi-insulating GaAs substrate with lateral dimensions of approximately 2×1 cm. The switch was triggered by focusing the pump beam on the open end of the transmission line. The rise time of the current is expected to be of the order of 1 ps (Ref. 2) while the decay time is determined by the recombination time of the GaAs substrate. A bias voltage of amplitude 20 V and frequency 2 kHz was applied to the transmission line. Figure 3(a) shows the results of current autocorrelation measurements.¹ The average current in the sense line was measured after being gated with the probe beam. In addition an oscilloscope⁵ was connected across a surface mount resistor in the main line in order to monitor the shape of the current pulses and confirm that the focused pump spot was in the optimum position. The rise time of the trace is limited by the bandwidth of the oscilloscope. Fits to the current autocorrelation measurements and the oscilloscope trace indicate that after the first few picoseconds the time dependent current is well described by the expression $I = I_0 \exp(-t/\tau)$, where I_0 and τ are approximately equal to 20 mA and 2 ns, respectively. The large value of τ means that the autocorrelation curve is rather insensitive to the rise time of the current and so its value cannot be reliably determined. All current autocorrelation and time resolved Kerr rotation measurements were made in a phase sensitive manner using the transmission line bias voltage as a reference.

The sample chosen for the present study was a 500 Å film of Fe grown by electron beam evaporation, at a background pressure of 10^{-6} mbar, onto a glass substrate and capped with a 300 Å layer of Au. The sample was placed face down on the transmission line structure and probed through the substrate. A piece of insulating tape of thickness 60 μm was placed between the sample and the switch to prevent the metallic sample from short circuiting the transmission line.

III. THEORY

The motion of the sample magnetization may be described by the Landau–Lifshitz–Gilbert equation of motion

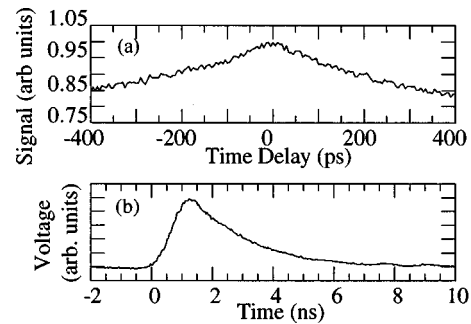


FIG. 3. (a) A typical current autocorrelation signal. (b) An oscilloscope trace indicating the time dependence of the current in the main line.

$$\frac{\partial \mathbf{M}}{\partial t} = -|\gamma| \mathbf{M} \times \mathbf{H}_{\text{eff}} + \frac{\alpha}{M} \left(\mathbf{M} \times \frac{\partial \mathbf{M}}{\partial t} \right), \quad (1)$$

where \mathbf{M} is the magnetization vector, γ is the magneto mechanical ratio, and α is the damping constant. The total effective magnetic field \mathbf{H}_{eff} includes the static applied magnetic field, the pulsed magnetic field \mathbf{h} , and the thin film demagnetizing field. The equation of motion may be solved numerically after being cast into a suitable form.⁶

The magneto-optical Kerr rotation of the reflected probe beam is dependent upon the components of the magnetization in the plane of incidence through the longitudinal and polar Kerr effects. Zak *et al.* have calculated expressions for the complex reflection coefficients r_{pp} and r_{sp} at the interface between a magnetic medium and a nonmagnetic medium for the case that the magnetization is canted relative to the interface.⁷ By combining the solution of Eq. (1) with Eqs. (19) and (22) of Ref. 7 we are able to calculate the time dependent Kerr rotation. This simple treatment may be applied to the present study because the thickness of the Fe film is large compared to the optical skin depth, and because multiple reflections in the glass substrate may be ignored due to the small value of the reflection coefficient at the air–glass interface.

IV. RESULTS

Measurements were performed with a static magnetic field of 1.04 kOe applied along the x axis in Fig. 2, i.e., parallel to the length of the transmission line and perpendicular to the plane of incidence. The probe beam was incident on the glass substrate at an angle of approximately 20° . The focused spot was scanned across the transmission line and the time dependent Kerr rotation recorded. It was necessary to subtract a background signal from the rotation data. We believe that the background is due to motion of the sample. This occurs because the static magnetic field exerts a force on the alternating current in the transmission line.

The lifetime of an individual current pulse is long compared to the time taken for the pulse to travel the length of the transmission line. The magnetic field associated with the current can therefore be calculated by assuming a uniform current density in the Au tracks and using the value of the current described in Sec. II. The pulsed magnetic field vector lies perpendicular to the length of the transmission line. At a height of 60 μm above the center of one of the Au tracks we

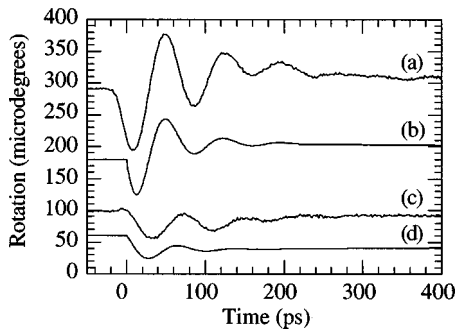


FIG. 4. The measured and calculated time dependent Kerr rotations are plotted for the case that the probe spot is: (a), (b) halfway between the two Au tracks; (c), (d) above the center of a Au track.

obtain peak field values of $|h_y|=0.48$ Oe and $|h_z|=0.12$ Oe, while at the same height above the center of the transmission line structure we obtain values of 0 and 0.53 Oe. The time dependent Kerr rotations measured for these two probe spot positions correspond to traces (a) and (c) in Fig. 4. Traces (b) and (d) were calculated by assuming: the values of the pulsed magnetic field above; bulk values of 2.09 and 1710 emu/cm³ for the g factor and the magnetization of the Fe film; a value of 0.1 for the damping constant α ; a value of 1.55 for the refractive index of glass; values of $3.03+3.69i$ and $0.0575-0.00768i$ for the refractive index⁸ and the magneto-optic constant⁹ of Fe; and an infinitesimally short rise time for the pulsed magnetic field. While the relative phase of the two experimental curves is expected to be correct, the absolute phase could not be accurately determined. Therefore the experimental data has been shifted so as to align the first maxima in curves (a) and (b) in Fig. 4. We see that the amplitude and frequency of the calculated curves are in reasonable agreement with the experimental data. The frequency of oscillation in the experimental data is approximately 13 GHz while in the calculation a frequency of 14.2 GHz is obtained as expected from the expression $\omega = \gamma\sqrt{H(H+4\pi M)}$. Better agreement between calculation and experiment might be obtained by varying the values of the material parameters and by allowing the pump field to have a finite rise time as in Ref. 3.

The calculated y and z components of the vector $\mathbf{u}=\mathbf{M}/M$ have been plotted in Fig. 5. The maximum deviation of the magnetization from the equilibrium position is seen to be an order of magnitude larger in Fig. 5(a) where the direction of the pulsed magnetic field vector lies close to the plane of the sample. The Kerr rotation depends upon u_y through the longitudinal Kerr effect and on u_z through the polar Kerr effect. Although the polar Kerr effect is an order of magnitude larger than the longitudinal Kerr effect in Fe, u_y is an order of magnitude larger than u_z in Fig. 5(a) and so u_y and u_z make contributions of similar magnitude to the total Kerr rotation in Fig. 4(a). However in Fig. 5(b) u_y and u_z are of similar magnitude and so u_z dominates the total rotation signal.

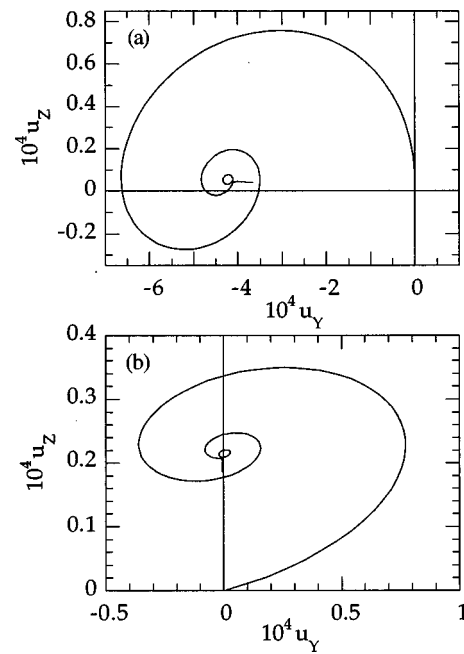


FIG. 5. The trajectories of the unit vector \mathbf{u} are plotted. Panels (a) and (b) correspond to the traces (b) and (d), respectively, in Fig. 4.

V. SUMMARY

In conclusion, we have observed FMR oscillations from a thin Fe film in the time domain. A photoconductive switch was used to apply the pump magnetic field both parallel and perpendicular to the plane of the sample. A larger deviation of the magnetization was achieved with the in-plane pump and we have found that it is essential to take account of both the longitudinal and polar Kerr effects when calculating the magneto-optical response of the sample. The calculated Kerr rotation is in reasonable agreement with the experimental curves given that the values of a large number of material parameters have been assumed.

ACKNOWLEDGMENTS

The authors gratefully acknowledge the support of the EPSRC and the LSF laser loan pool, the fabrication of samples by D. J. Jarvis, and discussions with Dr. C. D. H. Williams and Dr. T. W. Preist.

- ¹M. R. Freeman, R. R. Ruf, and R. J. Gambino, *IEEE Trans. Magn.* **27**, 4840 (1991).
- ²M. R. Freeman, M. J. Brady, and J. Smyth, *Appl. Phys. Lett.* **60**, 2555 (1992).
- ³W. K. Hiebert, A. Stankiewicz, and M. R. Freeman, *Phys. Rev. Lett.* **79**, 1134 (1997).
- ⁴J. A. C. Bland, M. J. Padgett, R. J. Butcher, and N. Bett, *J. Phys. E* **22**, 308 (1989).
- ⁵Tektronix DSA 601A with an 11A72 plug-in.
- ⁶L. He and W. D. Doyle, *J. Appl. Phys.* **79**, 6489 (1996).
- ⁷J. Zak, E. R. Moog, C. Liu, and S. D. Bader, *J. Appl. Phys.* **68**, 4203 (1990).
- ⁸*Handbook of Chemistry and Physics*, 75th ed. (Chemical Rubber, Boca Raton, 1994).
- ⁹G. S. Krinchik and V. A. Artem'ev, *Sov. Phys. JETP* **26**, 1080 (1968).